Static Aeroelastic Analysis of Fighter Aircraft Using a Three-Dimensional Navier-Stokes Algorithm

David M. Schuster*
Georgia Tech Research Institute, Atlanta, Georgia
and
Joseph Vadyak† and Essam Atta‡
Lockheed Aeronautical Systems Company, Burbank, California

An aeroelastic analysis method for fighter aircraft operating at extreme flight conditions has been developed and tested. The method involves the use of state-of-the-art zonal grid generation methods, three-dimensional Reynolds-averaged Navier-Stokes analysis, and linear structures to analyze the flow over complex, flexible aircraft. The main objective of this effort is to develop a method capable of analyzing aircraft operating at flight conditions where vortices, strong shock waves, separated flow, and even highly unsteady flow may be present. The present application focuses on the static aeroelastic analysis of fighter aircraft operating at high angle of attack and high transonic Mach number. The developed method has been compared against static aeroelastic wind-tunnel data on an aeroelastically tailored wing/fuselage configuration, and the results are very encouraging.

Introduction

A GREAT deal of emphasis is being placed on the development of accurate computational methods for the aeroelastic analysis of aircraft operating at extreme flight conditions. This capability is especially needed for the analysis of maneuvering fighter aircraft.

Modern fighters are increasingly called upon to operate at extreme flight conditions involving high lift coefficients and high transonic Mach numbers. In order to achieve and sustain flight in this regime, the wing is forced to operate in a highly transonic flow where, inevitably, strong shock waves and separated flow exist. In addition, aerodynamicists have been forced to utilize fluid dynamic phenomena like vortex flow so as to enhance wing performance at these conditions. These aerodynamic design techniques often lead to localized high loads, so that only small portions of the wing are generating the overall lift while the remaining portions are not heavily loaded. An accurate aeroelastic analysis technique is required to aid in identifying these areas so that the wing structure can be efficiently designed.

In addition to the basic aeroelastic analysis problem, there is a need for this type of technology from an aerodynamic/structural design standpoint. The development of composite technology has made the aeroelastic tailoring of lifting surfaces feasible. This is especially applicable to maneuvering fighter aircraft where high loads can be used to warp the lifting surface into a shape that will be aerodynamically favorable. Accurate prediction of flight loads is essential to the effective tailoring of the wing structure to deflect to a predetermined, aerodynamically efficient shape under maneuver loading.

Finally, it is becoming apparent that one of the most significant side effects of fighters operating under maneuvering conditions is the reduction in service life of tail surfaces due to fatigue. This fatigue is caused by buffet resulting from the bursting of strake and wing vortices. Burst vortices generally produce a highly unsteady flow that ultimately fatigues tail sections, especially the vertical fins of twin-tailed fighters. This problem requires an analysis capability applicable to unsteady, viscous dominated flows.

Unfortunately, the geometric and computational complexity of coupled aerodynamic/structural analysis has forced engineers to rely on simplified aerodynamics to solve aeroelastic problems. Programs like XTRAN3S[1] and CAP-TSD[2] utilize transonic small-disturbance aerodynamics to model static and dynamic aeroelastic problems. Although these methods are somewhat effective for problems involving relatively weak shock waves and attached flow, they simply cannot be applied to problems involving a maneuvering fighter, where viscous effects dominate the flow. Also, although these methods can be used to analyze complete aircraft configurations, surface boundary conditions are applied at a relatively crude approximation to the actual geometry. Therefore, accurate analyses of aircraft geometries that demonstrate a strong interaction between various aircraft components cannot be performed effectively using these methods. Modern fighter designs often rely on the aerodynamic interaction of the wing, fuselage, and, sometimes, a leading-edge strake to achieve the desired aerodynamic performance. Accurate prediction of the flowfields for these types of vehicles requires an accurate geometric model.

Researchers have realized for quite some time that effective analysis of these types of problems requires the development and application of three-dimensional Navier-Stokes technology. This is evidenced by the comments of the authors of Refs. 3 and 4. Until recently, however, numerical algorithms, modeling methods, and computer facilities capable of solving the Navier-Stokes equations for complex problems have not been available. This trend is rapidly changing due to developments like zonal grid generation methods and new supercomputer hardware.

For the past decade, Lockheed Aeronautical Systems Company has been heavily involved in the development and application of Navier-Stokes solvers to realistic aircraft problems. Reference 5 presents an overview of this development for a wide variety of aerodynamic configurations and problems. Reference 6 describes an application of the problem to a generic fighter geometry operating at high incidence involv-

Received Nov. 22, 1989; presented as Paper 90-0455 at the 28th Aerospace Sciences Meeting, Reno, NV, Jan. 8-11, 1990; revision received May 29, 1990; accepted for publication June 22, 1990.

*Research Engineer. Member AIAA.
†Senior Scientist. Member AIAA.
‡Scientist. Member AIAA.

ing a burst vortex. The favorable comparison of these calculations with experimental laser velocimeter data demonstrates the utility of this program for complex, viscous-dominated flows.

This paper describes the further application of this technology to the computation of flowfields about flexible fighter aircraft operating at extreme flight conditions. The developed method uses the Lockheed Euler/Navier-Stokes Three-Dimensional (ENS3D) aerodynamic method in conjunction with a zonal grid generation scheme and a linear structural model. The method has been programmed for both static and dynamic analysis, but to this point only the static analysis option has been tested. Turbulence characteristics for the program are supplied by the Baldwin-Lomax algebraic turbulence model of Ref. 7.

Grid Generation Method

In order to model complex aircraft geometries efficiently, a zonal H-grid topology has been chosen to model complete aircraft configurations for use in the aeroelastic method. This method allows the aircraft to be broken into logical components such as the wing, fuselage, etc., about which grids can be tailored to the individual pieces. The grid generation method is closely patterned after that described in Ref. 8 and is capable of modeling configurations consisting of combinations of wing, fuselage, canard, horizontal tail, and vertical tail. At the present time, the program only models vertical tails located in the plane of symmetry of the aircraft.

The method, known as the Complete Aircraft Mesh Program (CAMP), uses a hybrid algebraic/parabolic/elliptic grid generation scheme to generate grids in two-dimensional sections, which are subsequently stacked and algebraically sheared to develop the full three-dimensional grid. The parabolic scheme used in the program is that of Noack and Anderson.[9]

The zonal H-grid topology for a typical wing/fuselage grid is shown in Fig. 1. Basically, CAMP breaks up the configuration into a wing zone and a fuselage zone. Each of these zones is eventually subdivided into upper and lower zones. The wing zone contains all of the horizontal lifting surfaces. Therefore, the wing, canard, and horizontal tail are all modeled in the wing zone. The fuselage zone contains the fuselage and vertical tail.

The details surrounding the actual generation of the grid are described in Ref. 8 and will not be repeated here. It should be mentioned, however, that the program utilizes a modular input format so that different aircraft components can be readily added or deleted. The scheme is extremely efficient, especially after the addition of the parabolic grid generation scheme, which was not included in the original program. Generation of a four-zone, 318,000 grid point wing/fuselage grid requires only 11 s on a Cray X/MP-24.

Aeroelastic Method

The aeroelastic method is centered around Lockheed's ENS3D method. This program solves the three-dimensional Reynolds-averaged Navier-Stokes equations for compressible flow. The method, described in Refs. 5 and 6, uses an implicit time-stepping algorithm to advance the solution. The equations are written in strong conservation form for general curvilinear coordinates. The algorithm can be run in a time-accurate mode by using a fixed time step or in a steady-state mode using a spatially varying time step. All of the computations presented here were run using the steady-state option.

Flow data are passed from one grid zone to the next using linear interpolation and averaging. Although this method does not guarantee conservation of mass and momentum across the zonal interfaces, subsonic tests performed in Ref. 10 show no disturbance across zonal interfaces and results compare favorably with experimental data. Recent tests on transonic problems have generated similar results.

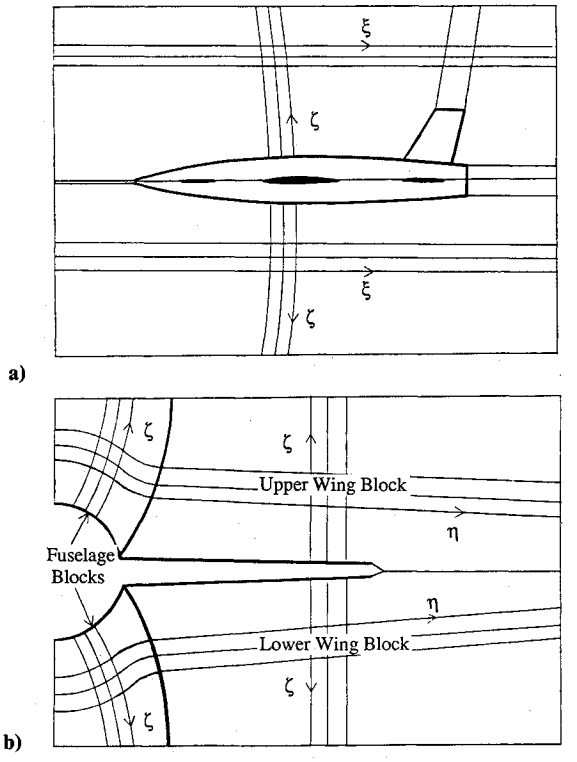

Fig. 1 Zonal H-grid topology.

This method uses one of two models to calculate the structural deflections. Both of these models result in the solution of a matrix equation of the form

$$[M]\{\ddot{q}\} + [D]\{\dot{q}\} + [K]\{q\} = \{F\} \tag{1}$$

where $[M]$ is a mass matrix, $[D]$ a damping matrix, and $[K]$ a stiffness matrix. The variables $\{q\}$, $\{\dot{q}\}$, and $\{\ddot{q}\}$ are vectors representing the structural deflection, the first time derivative of the deflection, and the second time derivative of the deflection, respectively; $\{F\}$ is a force vector of the form

$$\{F\} = \{F_A\} + \{F_I\} \tag{2}$$

where $\{F_A\}$ is the aerodynamic force vector calculated by ENS3D and $\{F_I\}$ is the inertial force vector determined from the flight condition (i.e., g loading).

The aeroelastic method has been written so that a fully dynamic analysis, including inertial loads, can be performed. However, all of the cases presented in this paper are static with no inertial loading. Therefore, the time derivative terms and the inertial force term are identically zero and the problem reduces to the following:

$$[K]\{q\} = \{F_A\} \tag{3}$$

Either a structural influence coefficient model or a mode shape model can be used to generate the structural deflections. For the influence coefficient model, $[K]$ is simply the stiffness influence coefficient matrix, whereas $\{q\}$ is the vector of structural deflections at the influence coefficient locations. In this case, $\{F_A\}$ is computed by lumping the calculated aerodynamic forces at the locations of the stiffness influence coefficients.

The mode shape model, on the other hand, assumes a deflection of the form

$$\{w\} = [\Phi]\{q\} \tag{4}$$

where $\{w\}$ is the vector of physical deflections, $[\Phi]$ is a matrix whose columns are the deflection modes, and $\{q\}$ is a vector of

multipliers for the mode shapes. For this case, the matrix $[K]$ is the generalized stiffness matrix given by

$$[K] = [\Phi_{ic}]^T[k][\Phi_{ic}] \tag{5}$$

where $[k]$ is the stiffness influence coefficient matrix and $[\Phi_{ic}]$ is the matrix of mode shapes interpolated at the locations of the structural influence coefficients.

Similarly, $\{F_A\}$ is now the generalized force vector given by

$$\{F_A\} = [\Phi_A]^T\{f_A\} \tag{6}$$

where $[\Phi_A]^T$ is the transpose of the matrix of mode shapes interpolated at the aerodynamic points and $\{f_A\}$ is the vector of aerodynamic loads calculated by ENS3D.

The choice of the structural model is a trade-off between computer time/storage requirements vs ease of implementation. Basically, although easier to implement for most cases, the influence coefficient model can require as much as an order of magnitude more points to describe accurately the structure as compared to the mode shape model, which may only require three or four modes. This will result in a greater storage requirement and more computer time to solve the structural equations. However, mode shapes are not always readily available, and the time and storage required for the structural analysis, even using the influence coefficient model, is minimal when compared to the aerodynamic analysis. It has been our experience that the influence coefficient model is easier to implement and has been found to produce very reliable results. Thus, it is generally worth the extra computer storage and execution time to use this model.

An important issue that ultimately influences the accuracy of the aerodynamic solution is the method used to update the grid to account for the structural deflection. The procedure developed for this method is a simple algebraic shearing that preserves the initial quality of the grid. Figure 2 will be used to describe the grid update method. It is assumed that all structural deflections are restricted to the Y direction, as defined in the figure. This approximation tends to stretch or compress the airfoil chord as the wing twists, but for a twist increment as large as 10 deg, the chord stretches less than 2%. Thus, for moderate deflections, this approximation has a minimal impact on the computed wing load.

The basic idea behind the grid deflection method is to update the grid so that points near the aeroelastic surface move with the surface, whereas points near the upper and lower boundaries do not move significantly. This is accomplished by computing a normalized arc-length distribution for each grid line connecting the aeroelastic surface to the top or bottom boundary. The deflection of each grid point along a given line is computed according to the following formula:

$$\Delta Y_K = \Delta Y_{ae}(1 - S_K/S_{max}) \tag{7}$$

where ΔY_{ae} is the deflection at the aeroelastic surface, S_K the arc length along the grid line at point K, and S_{max} the total arc length for the grid line. Grid points ahead of and behind the aeroelastic surface are updated according to the deflection of the leading and trailing edge of the surface, respectively. Points beyond the wingtip are handled similarly.

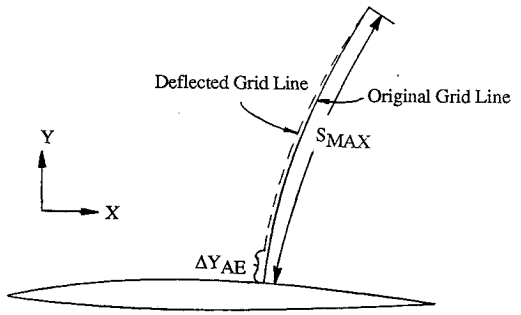

Fig. 2 Grid deflection method.

Although this is an extremely simple method for updating the grid, it is also very effective. The procedure tends to maintain the quality of the initial grid, especially near the aeroelastic surface where resolution of the boundary layer is important. The method guarantees that grid lines will not cross as long as the surface is not deflected past the upper or lower boundary of the grid. It also ensures that if the original grid was smooth and the deflection distribution is smooth, then the deflected grid will be smooth.

Analysis Results

The aeroelastically tailored wing/fuselage configuration of Ref. 11 was used to test the ENS3D aeroelastic method. The washout wing design of this study was chosen for this analysis. This wing was designed for operation at 0.9 Mach number, a Reynolds number of 7×10^6 based on the wing chord at the intersection of the strake and wing (10,000-ft altitude), and a lift coefficient of 0.7. These conditions are representative of a fighter aircraft performing a 9 g maneuver. The angle of attack for these conditions is approximately 9 degs for the washout wing. All numerical test cases were run at these conditions.

The tested configuration consists of a swept, tapered wing with a symmetrical airfoil section, an axisymmetric fuselage, and a leading-edge strake. The planform of the configuration is shown in Fig. 3. Experimental data for this model include force data, static pressure data, and measured aeroelastic deflections. Both a wing alone and the complete wing/fuselage/strake configuration were tested in the present analysis.

The grid generated for this configuration consists of a total of four zones and approximately 318,000 grid points. The leading-edge strake is modeled as part of the fuselage, and

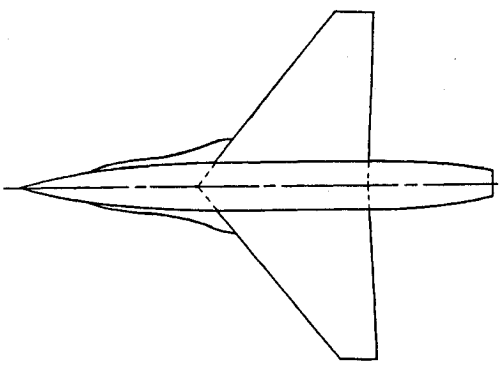

Fig. 3 Planform view of the aeroelastically tailored fighter wing/body.

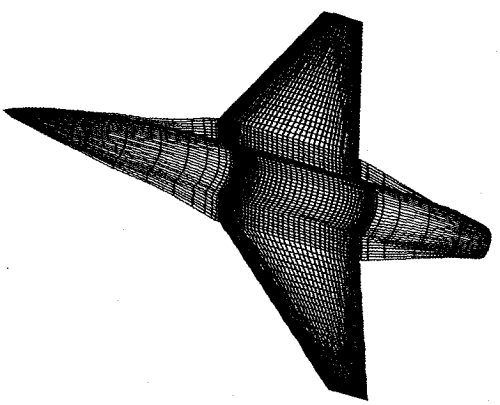

Fig. 4 Surface grid for the aeroelastically tailored fighter wing/body.

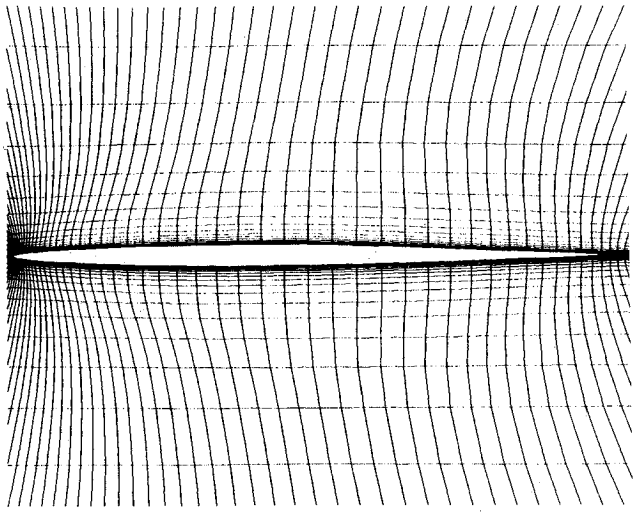

Fig. 5 Wing section H-grid.

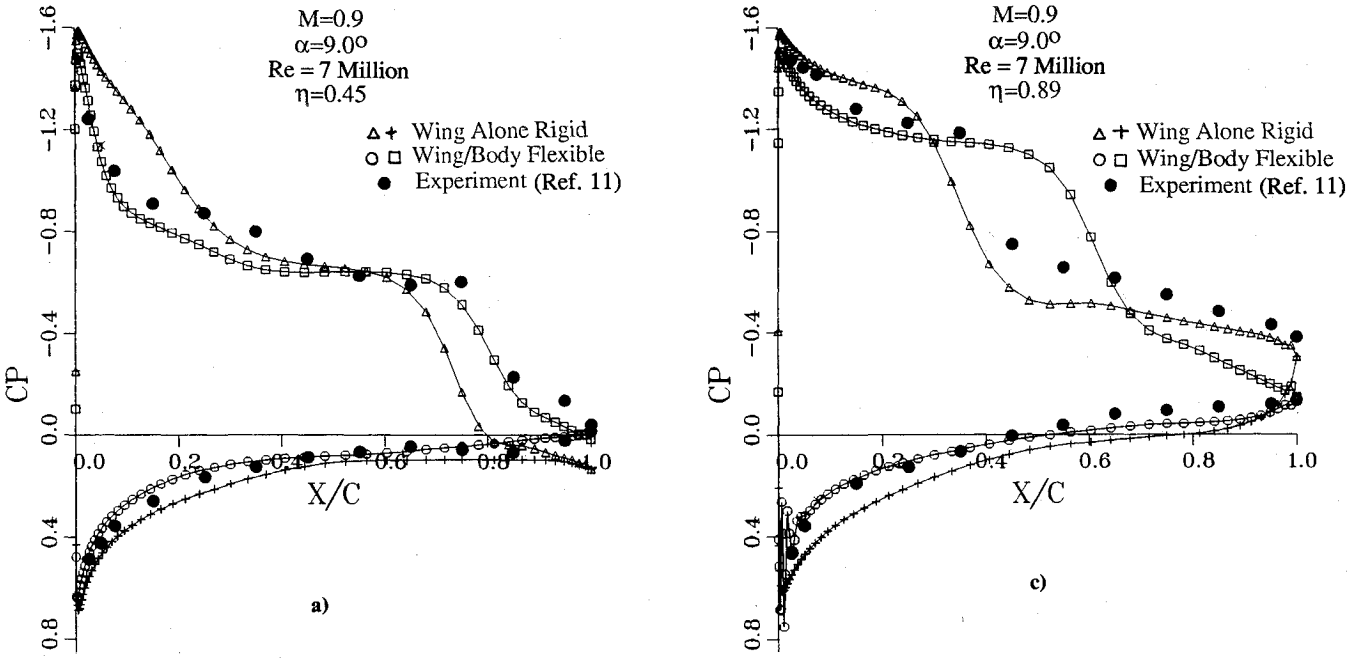

Fig. 6 Computed and experimental pressure distributions for the aeroelastically tailored fighter.

there are a total of 22 spanwise stations between the fuselage symmetry plane and the wing/strake intersection and 25 stations on the wing. The grid extends four wing root chords ahead of the fuselage nose and six root chords downstream of the aft-most point on the fuselage. The upper and lower boundaries are located four root chords above and below the wing midplane, and the spanwise boundary is located two wing semispans from the fuselage symmetry plane.

Figure 4 presents the surface grid generated for this geometry. As can be seen in the figure, a trailing-edge bat has been added to the aft fuselage. This section allows the fuselage grid to have a smooth transition from the spanwise location where the leading-edge strake intersects the wing to the aft fuselage. Although the addition of this bat adds lifting area and will ultimately impact the overall configuration loads, it will not have a significant impact on the wing surface pressure distributions. The high transonic Mach numbers at which the analysis is being performed will tend to shield the area forward of the bat from any disturbance it may generate. The loads on any portion of the body inboard of the wing/strake/bat intersection are not included in the aeroelastic analysis of the wing (i.e., these components are assumed rigid), and so addition of this approximation to the geometry will not have a significant impact on the overall aeroelastic results. A second grid omitting the fuselage and strake was also generated to perform initial tests of the method and to determine the sensitivity of the analysis at these flow conditions to accurate geometric modeling.

Figure 5 shows a grid about a wing section of the model. The grid is highly clustered near the airfoil surface so as to resolve the boundary layer. The first grid point is placed 0.0005 local chords from the airfoil surface, representing a y^+ of approximately 7.8 at the point of maximum surface shear. A hyperbolic sine distribution function is used to stretch the grid to the upper and lower boundaries. There are a total of 32 grid points normal to the airfoil surface.

A Cray X/MP-24 computer was used for all of the subsequent calculations. The computer used in the analysis is equipped with a solid-state storage device (SSD) on which each grid block and associated flow variables were temporarily stored. Each 92 × 32 × 32 (94,208 points) wing grid block requires approximately 3.8 of the 4 × 10^6 words of core storage to execute in the aeroelastic program. Therefore, each grid and flowfield block is transferred in and out of core via the SSD for each time step in the analysis. The SSD is extremely efficient, and input/output to this device accounts for less than 1% of the overall computation time. The 318,000 grid point case requires approximately 8 h of Cray CPU time to complete 1000 time steps in the analysis.

A number of cases involving rigid and flexible analyses of the wing alone and wing/fuselage configuration were performed. Figures 6 compare computed pressure distributions for the rigid wing alone and flexible wing/body analyses with experimental data. These data demonstrate the cumulative error that can be incurred by neglecting both accurate geometry modeling and the effect of structural flexibility. Figure 6a presents the comparison at 45% of the wing semispan. At this station we see that the flowfield has basically the same overall character, but the flexible wing/body analysis compares much better with the experimental data at all points on the airfoil. ENS3D does an exceptional job of predicting the leading-edge pressure distribution, the shock location, and the lower surface pressures.

Figure 6b compares the pressures at 60% span. There is a significant difference in the character of the flow between the rigid wing alone analysis and the flexible wing/body analysis at this station. Once again, the flexible ENS3D analysis compares very well with the experimental pressures. The leading-edge pressure, shock location, and lower surface pressure are all well predicted.

Finally, Fig. 6c compares the pressures at 89% span. Except for a small pressure oscillation near the wing leading edge, ENS3D does a good job of predicting the lower surface pressure. The correlation on the upper surface, however, is not as good as for previous stations. The pressures near the leading edge are well predicted, but the shock is pushed well aft of the experimental shock location. The experimental pressures are indicating massive upper surface flow separation, but the flexible ENS3D analysis does not seem to capture this.

This can be attributed to a combination of two factors. First, as the washout wingtip deflects upward, the local angle of attack at this station is reduced. Thus, the flexible wing will not tend to separate at the tip as early as the rigid wing. This characteristic is obviously captured by the present method since only mild separation is indicated in the flexible wing pressures.

The fact that the flexible Navier-Stokes analysis does not predict the large extent of upper surface flow separation can be attributed to the turbulence model employed in the analysis. The Baldwin-Lomax turbulence model does not account for the streamwise turbulence history of the flow. This typically causes the model to overpredict the turbulence quantities at downstream locations, causing flows to remain attached longer than experimentally observed. The rigid wing alone solution accurately predicts the massive upper surface flow separation, and the shock location and pressures correlate very well with the experimental data. This indicates that implementation of a turbulence model better suited to capturing separated flow would produce improved results near the wingtip.

For reference, Fig. 7 compares the rigid wing/body pressures with the flexible wing/body pressures and experimental data at the 60% span station. As expected for the washout wing, the addition of flexibility to the analysis tends to reduce the suction level near the wing leading edge and lowers the pressure on the lower surface. Both of these trends are indicative of a decrease in the angle of attack, which is what is expected for a washout wing under these conditions.

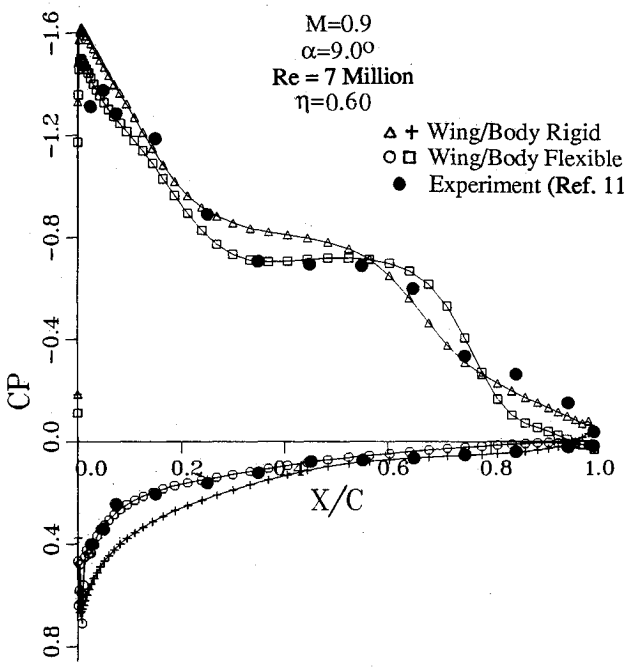

Fig. 7 Comparison of wing/body flexible and wing/body rigid pressures for the aeroelastically tailored fighter.

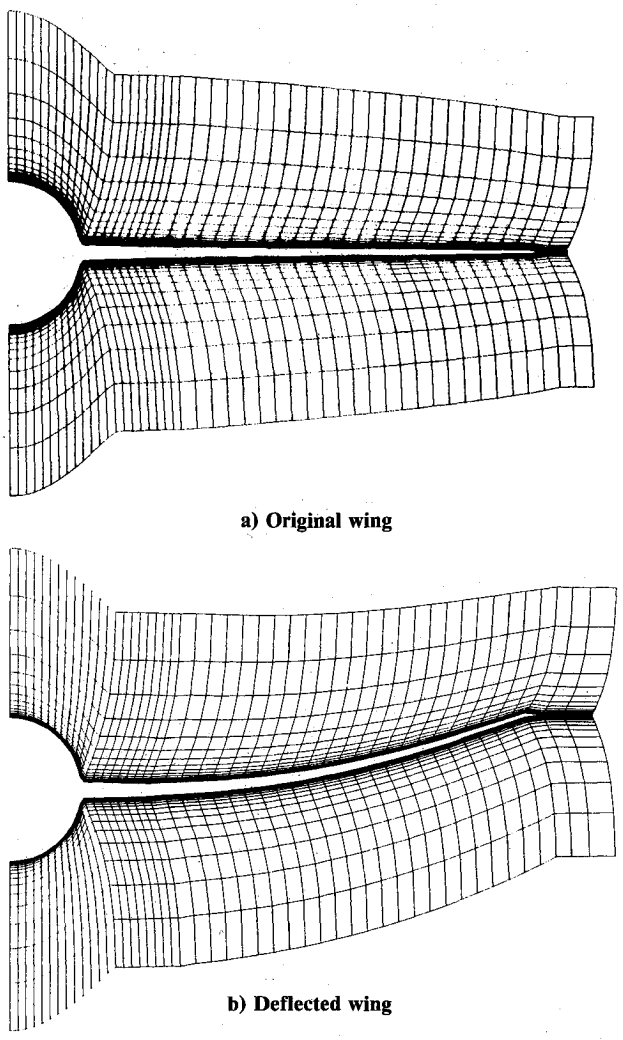

Fig. 8 Front view of the original and deflected wing/fuselage grid.

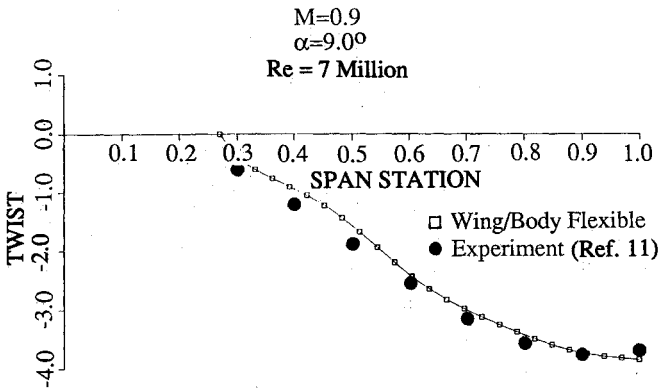

Fig. 9 Wing twist distribution comparison for the aeroelastically tailored fighter.

Figures 8 show a front view of a section of the wing/body grid before and after it has been deflected by the aeroelastic analysis. These figures are presented for two reasons. First, they show the effectiveness of the grid update procedure employed in the aeroelastic analysis. This grid has been deflected over a thousand times (once every time step) and there has been no degradation to the grid over this period. The grid is still well clustered near the wing surface and it is smooth everywhere. The second reason is to illustrate the extent to which this wing has flexed. The original wing was flat, i.e., no leading-edge deflection and no twist. The experimental data indicate a front spar deflection of 3 in. at the wingtip and ENS3D predicts a deflection of 2.8 in. at this station. The wing semispan for the model was approximately 22 in. and as can be seen, the deflection for this case is significant.

A comparison of the computed and experimental wing twist distributions is shown in Fig. 9. Once again, excellent agreement with the experimental data is obtained. ENS3D predicts the wing twist within 0.1 deg over virtually the entire wing semispan. The structural model for this analysis consisted of only four chordwise and seven spanwise stations. This demonstrates the ability of ENS3D to produce accurate results using a computationally efficient structural model.

Conclusions

A three-dimensional Navier-Stokes solver has been coupled with a linear structural model and a zonal grid generation scheme to provide aeroelastic analyses of aircraft operating at extreme flight conditions. The method has been tested on an aeroelastically tailored wing/body configuration representative of modern fighter aircraft. Flow conditions for these tests are typical of those experienced by fighter aircraft operating in a 9 *g* maneuver. The developed method compares very well with experimentally measured data both from a fluid dynamics and structural deflection standpoint. The analyses demonstrate the effectiveness of the numerical solution of the Navier-Stokes equations in solving these types of problems. In addition, the importance of an accurate geometric model for effective analysis at these flight conditions is also demonstrated. Turbulence modeling has been shown to delay the prediction of upper surface flow separation for the flexible wing/fuselage case, indicating that further work must be performed in this area.

Acknowledgments

This effort has been sponsored by Air Force Wright Aeronautical Laboratories Contract 33615-87-C-3209, "Flight Loads Prediction Methods for Fighter Aircraft." The authors would like to express their appreciation to Elijah Turner and Larry Huttsell of WRDC/FIB for their continuous support throughout this program. They would also like to thank John Malone of NASA Langley Research Center for his insight and ideas that aided in the development of this method.

References

[1]Borland, C. J., and Rizetta, D. P., "Nonlinear Transonic Flutter Analysis," *AIAA Journal,* Vol. 20, No. 11, 1982, pp. 1600–1615.

[2]Batina, J. T., Seidel, J. A., Bland, S. R., and Bennett, R. M., "Unsteady Transoniv Flow Calculations for Realistic Aircraft Configurations," AIAA Paper 87-0850, April 1987.

[3]Edwards, J. W., and Thomas, J. L., "Computational Methods for Unsteady Transonic Flows," AIAA Paper 86-0107, Jan. 1987.

[4]Whitlow, W., "Computational Unsteady Aerodynamics for Aeroelastic Analysis," NASA TM-100523, Dec. 1987.

[5]Vadyak, J., Smith, M. J., Schuster, D. M., and Shrewsbury, G. D., "Simulation of Aircraft Component Flowfields Using a Three-Dimensional Navier-Stokes Algorithm," *Proceedings of the 3rd International Symposium on Science and Engineering on Cray Supercomputers,* Cray Research, Inc., Minneapolis, MN, Sept. 1987, pp. 141–167.

[6]Vadyak, J., and Schuster, D. M., "Navier-Stokes Simulation of Burst Vortex Flowfields for Fighter Aircraft at High Incidence," AIAA Paper 89-2190, July 1989.

[7]Baldwin, B. S., and Lomax, H., "Thin Layer Approximation and Algebraic Model for Separated Turbulent Flows," AIAA Paper 78-257, Jan. 1978.

[8]Atta, E., Birckelbaw, L., and Hall, K., "Zonal Grid Generation Method for Complex Configurations," *Journal of Aircraft,* Vol. 25, No. 10, 1988, pp. 911–913.

[9]Noack, R. W., and Anderson, D. A., "Solution Adaptive Grid Generation Using Parabolic Partial Differential Equations," AIAA Paper 88-0315, Jan. 1988.

[10]Schuster, D. M., and Birckelbaw, L. D., "Numerical Computation of Viscous Flowfields About Multiple Component Airfoils," AIAA Paper 85-0167, Jan. 1985.

[11]Rogers, W. A., Braymen, W. W., and Shirk, M. H., "Design, Analyses, and Model Tests of an Aeroelastically Tailored Lifting Surface," *Journal of Aircraft,* Vol. 20, No. 3, 1983, pp. 208–215.